

## Evidence of the Zn Vacancy Acting as the Dominant Acceptor in *n*-Type ZnO

F. Tuomisto,\* V. Ranki, and K. Saarinen

*Laboratory of Physics, Helsinki University of Technology, P.O. Box 1100, 02015 HUT, Finland*

D C. Look

*Semiconductor Research Center, Wright State University, Dayton, Ohio, USA*

(Received 17 June 2003; published 10 November 2003)

We have used positron annihilation spectroscopy to determine the nature and the concentrations of the open volume defects in as-grown and electron irradiated ( $E_{\text{el}} = 2 \text{ MeV}$ , fluence  $6 \times 10^{17} \text{ cm}^{-2}$ ) ZnO samples. The Zn vacancies are identified at concentrations of  $[V_{\text{Zn}}] \approx 2 \times 10^{15} \text{ cm}^{-3}$  in the as-grown material and  $[V_{\text{Zn}}] \approx 2 \times 10^{16} \text{ cm}^{-3}$  in the irradiated ZnO. These concentrations are in very good agreement with the total acceptor density determined by temperature dependent Hall experiments. Thus, the Zn vacancies are dominant acceptors in both as-grown and irradiated ZnO.

DOI: 10.1103/PhysRevLett.91.205502

PACS numbers: 61.72.Ji, 61.82.Fk, 72.80.Ey, 78.70.Bj

Because of recent progress in crystal growth [1] and unique optical and electrical properties, zinc oxide (ZnO) can be considered as an alternative to gallium nitride (GaN) for use in optoelectronic devices. It crystallizes in the wurtzite structure and has a direct band gap of 3.437 eV at 2 K, similarly to GaN. Experiments have shown [2] that ZnO is significantly more radiation hard than Si, GaAs, or GaN, and should thus be more useful for applications in high-irradiation environments, such as electronics in space satellites.

Identification and quantification of point defects is important both for the electronic and optoelectronic applications, as well as for understanding the microscopic origin of the radiation hardness. Recent experimental studies [3,4] have shown that the dominant native shallow donor in ZnO is hydrogen (H), as predicted by calculations [5]. These studies show the presence of another shallow donor, the identity of which remains unknown. The dominant native acceptor defect has been predicted to be the zinc vacancy ( $V_{\text{Zn}}$ ) [6,7], but no experimental proof exists.

In this Letter, we apply positron annihilation spectroscopy to identify as well as quantify the open volume defects in both as-grown and electron irradiated ZnO. Positrons get trapped at vacancy defects, which changes their annihilation characteristics. The positron lifetime reflects the open volume of the defect. The Doppler broadening of the annihilation radiation gives information about the electron momentum distribution at the annihilation site and is sensitive to the atomic environment of the vacancy. The combination of these techniques thus allows the identification of both the open volume and the sublattice of the defect. In ZnO, preliminary results exist both in bulk crystals and epitaxial layers [8–10]. In this Letter, we show that the open volume defect produced by electron irradiation is the same as the dominant defect in as-grown ZnO, i.e., the Zn vacancy ( $V_{\text{Zn}}$ ). The Zn vacancies act as acceptors, and their concentration is suffi-

ciently high to explain the total acceptor density in both as-grown and irradiated ZnO.

We studied nominally undoped bulk ZnO crystals grown by the seeded vapor phase technique [1]. For the study of irradiation-induced defects, two samples were irradiated with 2 MeV electrons with fluence  $6 \times 10^{17} \text{ cm}^{-2}$ . The acceptor densities in the samples were determined by temperature dependent Hall measurements [11], where the mobility data is analyzed by fitting to it the solution of the Boltzmann transport equation [1]. Assuming a single-acceptor model, these analyses give  $N_A \approx 5 \times 10^{15} \text{ cm}^{-3}$  for the as-grown material and  $N_A \approx 7 \times 10^{16} \text{ cm}^{-3}$  for the irradiated material. Also the Fermi levels in the samples could be deduced from the data, giving  $E_C - E_F = 0.1 \text{ eV}$  for the as-grown sample and  $E_C - E_F = 0.2 \text{ eV}$  for the irradiated sample.

The positron annihilation experiments were performed at 10–500 K in the as-grown samples and at 10–300 K in the irradiated samples, using a conventional fast-fast spectrometer in collinear geometry [12] with a time resolution of 250 ps. In this scheme the 10  $\mu\text{Ci}$  positron source ( $^{22}\text{Na}$  deposited on 1.5  $\mu\text{m}$  Al foil) is sandwiched between two identical sample pieces. The lifetime spectrum  $n(t) = \sum_i I_i \exp(-t/\tau_i)$  was analyzed as the sum of exponential decay components convoluted with the Gaussian resolution function of the spectrometer, after subtracting the constant background and annihilations in the source material (200 ps, 2.0%; 400 ps, 3.9%; 1500 ps, 0.21%). The positron in state  $i$  annihilates with a lifetime  $\tau_i$  and an intensity  $I_i$ . The state in question can be the delocalized state in the lattice or the localized state at a vacancy defect. The increase of the average lifetime  $\tau_{\text{ave}} = \sum_i I_i \tau_i$  above the bulk lattice lifetime  $\tau_B$  shows that vacancy defects exist in the samples. The Doppler broadening of the annihilation radiation was measured using a Ge detector with an energy resolution of 1.3 keV. The coincidence detection of both 511 keV photons emitted from the positron-electron annihilation was

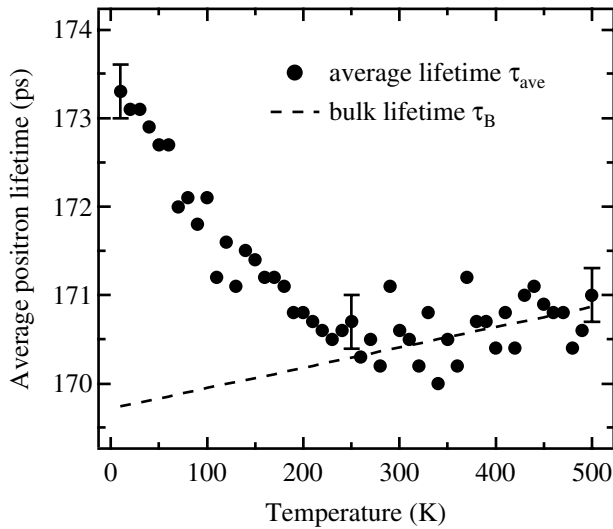


FIG. 1. The average positron lifetime of the as-grown ZnO sample as a function of the measurement temperature. The dashed line shows the temperature dependence of the positron lifetime in the ZnO lattice.

accomplished with a NaI detector providing the gate signal. The peak-to-background ratio was about  $10^4$  and  $3 \times 10^6$  counts were collected in the spectrum in the coincidence mode.

The average positron lifetime measured from the as-grown ZnO sample is shown as a function of the measurement temperature in Fig. 1. At 300–500 K the average positron lifetime in the as-grown sample is constant or very slightly increasing due to the thermal expansion of the lattice. It provides the lifetime of the positron in the delocalized state in the ZnO lattice,  $\tau_B = 170$  ps at 300 K. The increase in the average positron lifetime with decreasing temperature at 10–300 K is a clear indication of the presence of negatively charged vacancies, the positron trapping coefficient of which increases with decreasing temperature. The lifetime spectrum could be decomposed into two lifetime components at 10 K, giving  $\tau_2 = 265 \pm 25$  ps for the higher component. The large uncertainty in  $\tau_2$  is due to the fact that the increase in  $\tau_{\text{ave}}$  is very small, only 3 ps, because of the small intensity  $I_2$ .

The same increase in the average positron lifetime with decreasing temperature at 10–300 K is observed in the irradiated sample (Fig. 2). Here  $\tau_{\text{ave}}$  is clearly above the bulk value  $\tau_B$  and thus the decomposition of the lifetime spectra could be performed with much greater accuracy. The higher lifetime component  $\tau_2$  of the irradiated sample is presented in the upper part of Fig. 2, the average value is  $\tau_2 = 230 \pm 10$  ps, within experimental accuracy the same as  $\tau_2 = 265 \pm 25$  ps.

Doppler broadening measurements were performed to further identify the sublattice to which the defect belongs. The conventional valence ( $S$ , low momenta:  $|p_z| < 3 \times 10^{-3} m_0 c$ ) and core ( $W$ , high momenta:  $10 < |p_z| < 30 \times 10^{-3} m_0 c$ ) annihilation parameters determined from the

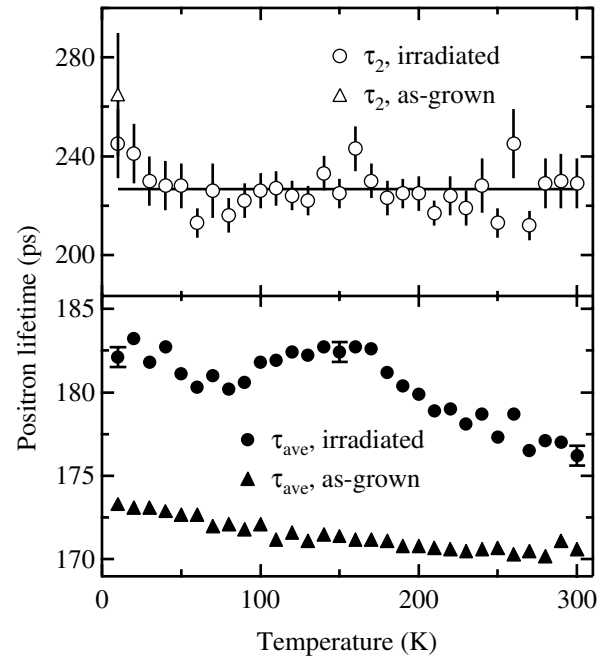


FIG. 2. The average positron lifetime of the as-grown and electron irradiated ZnO samples as a function of the measurement temperature. The higher lifetime component corresponding to positrons trapped at vacancies is shown in the top panel.

irradiated and as-grown samples at temperatures 10–300 K fall on a line in the  $S$  vs  $W$  plot. This implies that there is only one type of vacancy defect present [12]. Defects with no open volume produce the same annihilation parameters as the bulk lattice and are thus not observed in the slopes of the  $S$  vs  $W$  plot. The  $S$  and  $W$  parameters of the bulk lattice were determined from the as-grown sample in the temperature region 300–500 K. The characteristic  $S_D$  and  $W_D$  parameters of the vacancy defect could be determined from the irradiated sample data by fitting the equation for the fraction of annihilations at defects  $\eta_D = (\tau_{\text{ave}} - \tau_B)/(\tau_D - \tau_B) = (S - S_B)/(S_D - S_B) = (W - W_B)/(W_D - W_B)$  to the  $S(W)$  data. The scaled  $S$  and  $W$  parameters of the defect were obtained as  $S_D/S_B = 1.039(4)$  and  $W_D/W_B = 0.87(3)$ .

The obtained experimental values of  $\tau_D/\tau_B$ ,  $S_D/S_B$ , and  $W_D/W_B$  for the defect in ZnO can be compared to the corresponding values in GaN. The comparison is shown in Table I. From these values the defect observed in both as-grown and irradiated ZnO can be identified as the zinc vacancy  $V_{\text{Zn}}$ . This is also supported by the fact that 2 MeV electron irradiation with similar fluence as in this work is known to produce Ga vacancies in GaN [15]. Furthermore, since the oxygen vacancy  $V_{\text{O}}$  is a donor [11], the negative charge state of the observed defect implies that it is not  $V_{\text{O}}$ .

In the coincidence setup of the Doppler broadening measurements the peak-to-background ratio is low

TABLE I. Comparison of experimental and computational vacancy-related parameters in GaN and ZnO. The values for GaN are taken from Refs. [13,14].

	$\tau_D/\tau_B$	$S_D/S_B$	$W_D/W_B$
$V_X$ , exp., ZnO	1.35(5)	1.039(4)	0.87(3)
$V_{Ga}$ , exp., GaN	1.47(5)	1.038(2)	0.86(2)
$V_N$ , exp., GaN	1.13(5)		
$V_{Zn}$ , calc., ZnO	1.34(1)		0.890(1)
$V_O$ , calc., ZnO	1.02(1)		0.998(1)

enough to allow more accurate analysis of the high momentum region of the momentum distribution. Figure 3 presents the momentum distribution measured from the as-grown sample at 300 K, representing the bulk distribution, and two defect-specific distributions separated from the spectra measured at 10 and 150 K from the irradiated sample by the help of the annihilation fraction  $\eta_D$  and lifetime data. The core electron momentum distribution at the defect is clearly the same at both temperatures, indicating that the dominant defect is the same. In the case of the as-grown sample, the defect-specific momentum distribution could not be separated due to the low intensity of the second lifetime.

We calculated the positron lifetimes and core electron momentum distributions by solving the positron state and constructing the electron density of the wave function of the free atoms, similarly as described in Ref. [16]. The calculated momentum distributions for the bulk state, the

oxygen vacancy ( $V_O$ ), and the zinc vacancy ( $V_{Zn}$ ) are presented in the upper part of Fig. 3. The ions around the vacancies were positioned according to relaxations calculated in Ref. [7], i.e., inward relaxation of 7.7% of the Zn ions around  $V_O$  and outward relaxation of 8.8% of the O ions around  $V_{Zn}$ . The results show clearly that the core electron momentum distribution at  $V_O$  is indistinguishable from the distribution in the perfect lattice. On the other hand, the effect of the defect in the measured spectra is the same as the one of  $V_{Zn}$  in the calculated spectra, thus the defect can be identified as  $V_{Zn}$ . Also the calculated  $W_D/W_B$  values shown in Table I indicate that the vacancy belongs to the Zn sublattice. The same conclusion is reached also by investigating the differences  $W_D - W_B$ .

Further evidence of the Zn vacancy is obtained from the calculated lifetimes. The calculated bulk ZnO lifetime is  $\tau_B^c = 177$  ps. The calculated lifetimes of the vacancies are  $\tau_{V,O}^c = 180$  ps and  $\tau_{V,Zn}^c = 237$  ps. Similarly to the Doppler spectra, the lifetime of the O vacancy suggests that the positron localization is very weak at this defect. The calculated bulk lifetime is slightly higher than the measured one, but the most important quantity is the relative lifetime  $\tau_V/\tau_B$ . These values are tabulated in Table I and they are in very good agreement with the defect lifetimes obtained from the as-grown and irradiated ZnO samples. The positron lifetime was calculated also for the divacancy  $V_{Zn} - V_O$ . Because of the lack of accurate relaxation data, the calculations were performed for the ideal defect. The calculated lifetime was 34 ps higher than that of the single Zn vacancy, and in the case of probable outward relaxation (as for  $V_{Zn}$ ), the difference would be even larger. In the case of as-grown ZnO the possibility of  $V_{Zn}$  belonging to the divacancy  $V_{Zn} - V_O$  cannot be completely excluded. However, the  $(S, W)$  parameters measured from the as-grown sample fall on the same line with the ones measured from the irradiated sample, which supports strongly the identification of the defect as the zinc vacancy and not  $V_{Zn} - V_O$ . Thus it can be concluded that the observed defect in both irradiated and as-grown ZnO is the Zn vacancy. The above measured and calculated lifetimes also imply that most of the Zn vacancies are empty, i.e., they do not contain hydrogen impurities.

The form of the  $\tau_{ave}$  vs  $T$  curve of the as-grown sample (Fig. 1) is in good accordance with the  $T^{-1/2}$  temperature dependence [12] of the positron trapping coefficient at a negative vacancy defect. Assuming a specific trapping coefficient of  $\mu_V = 3 \times 10^{15} s^{-1}$  at 300 K as for the Ga vacancy in GaN [15], and scaling it to 10 K, the zinc vacancy concentration in the as-grown sample could be calculated from  $[V_{Zn}] = N_{at} \mu_V^{-1} \tau_B^{-1} (\tau_{ave} - \tau_B) / (\tau_D - \tau_{ave})$ , where  $\tau_{ave}$  and  $\tau_B$  are taken at 10 K, and  $\tau_D = \tau_2$  and the atomic density  $N_{at} = 8.3 \times 10^{22} cm^{-3}$ . This results in a zinc vacancy concentration of  $[V_{Zn}] \approx 2 \times 10^{15} cm^{-3}$ .

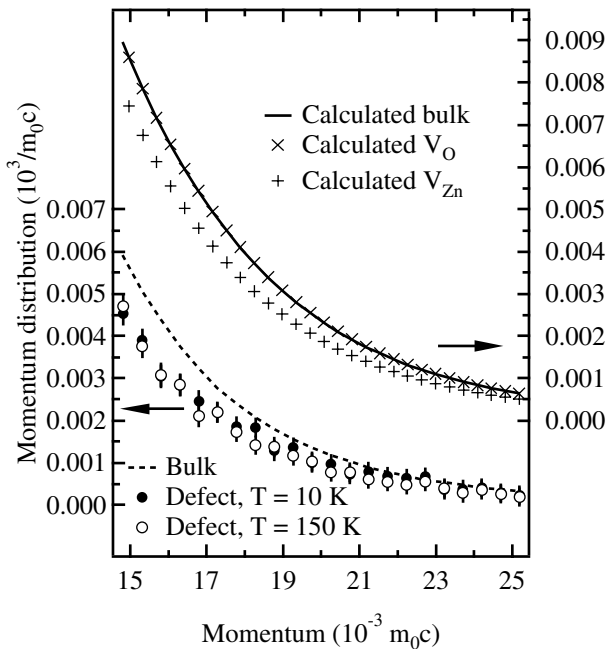


FIG. 3. Lower part: the measured core electron momentum distributions at the defect and in the perfect lattice. Upper part: the calculated core electron distributions at the oxygen vacancy, zinc vacancy, and in the perfect lattice.

On the other hand, the  $\tau_{\text{ave}}$  vs  $T$  curve of the irradiated sample at temperatures below  $T = 150$  K suggests that there is also another type of charged defect present in the material, with  $\tau_D < \tau_2$ . This defect thus has little or no open volume, i.e., it has the characteristics of a negative ion impurity or possibly the oxygen vacancy. Based on the observation that at temperatures above  $T = 150$  K the  $\tau_{\text{ave}}$  vs  $T$  curve is dominated by the  $T^{-1/2}$  behavior, it can be concluded that the negative ion is a shallow trap [12] from which positrons are able to escape thermally at these temperatures. According to theory [7], intrinsic defects like the interstitial oxygen ( $O_i$ ) and the oxygen antisite ( $O_{\text{Zn}}$ ) are negative in  $n$ -type ZnO and serve as prominent candidates for the negative ion introduced by electron irradiation.

The zinc vacancy concentration in the irradiated sample can be calculated in the same way as for the as-grown sample, but from the data in the temperature range  $T = 150$ – $300$  K, giving  $[V_{\text{Zn}}] \approx 2 \times 10^{16} \text{ cm}^{-3}$ . An estimate of the concentration of the negative ions can also be given, assuming a trapping coefficient  $\mu(T) \approx 7 \times 10^{16}(T/\text{K})^{-0.5} \text{ s}^{-1}$  [17] and applying a trapping model with two defects [12] at temperatures below  $T = 50$  K, where the detrapping is weak. The result is  $c_{\text{ion}} \approx 2 \times 10^{16} \text{ cm}^{-3}$ .

The only negative defect observed by positrons in the as-grown ZnO sample is the zinc vacancy, thus indicating that it is the dominant acceptor. According to calculations in Ref. [7], the doubly negatively charged state of the zinc vacancy ( $V_{\text{Zn}}^{2-}$ ) has the lowest formation energy when the Fermi level is near the bottom of the conduction band. Thus the zinc vacancies in the studied samples are mostly in this state. Hence, the Hall data should be analyzed with a double-acceptor model, where the fitted concentration of ionized centers is defined as  $N_I = 4N_{A^{2-}} + N_{D^+}$  instead of  $N_I = N_{A^-} + N_{D^+}$ . The free electron concentration obtained directly from the Hall measurements is  $n = N_{D^+} - 2N_{A^{2-}}$  in the case of double acceptors, resulting in  $N_I = 6N_{A^{2-}} + n$  as opposed to  $N_I = 2N_{A^-} + n$  in the single-acceptor model, thus reducing the acceptor concentration estimated from the Hall data by a factor of 3. This gives  $N_A \approx 1.7 \times 10^{15} \text{ cm}^{-3}$  in as-grown ZnO, which is in perfect agreement with the positron result for the zinc vacancies, i.e.,  $N_A^{V_{\text{Zn}}} \approx 2 \times 10^{15} \text{ cm}^{-3}$ .

In the irradiated sample the agreement between the Hall data analyzed with the double-acceptor model and the positron data is also very good. The total acceptor concentration is  $N_A \approx 2.3 \times 10^{16} \text{ cm}^{-3}$  and the acceptor density due to the zinc vacancies is  $N_A^{V_{\text{Zn}}} \approx 2 \times 10^{16} \text{ cm}^{-3}$ . Adding singly negative ions with concentration  $2 \times 10^{16} \text{ cm}^{-3}$  to the double-acceptor model indicates that their contribution to the total acceptor density should be 25%, which is in very good agreement with the results of the positron experiments which indicate a value of about 33%. Thus, our results show that the zinc va-

cancy is the dominating acceptor defect both in as-grown and in electron irradiated ZnO. However, the negative ion defects (tentatively attributed to  $O_i$  and/or  $O_{\text{Zn}}$ ) also contribute in irradiated material.

The relatively low vacancy concentration in 2 MeV electron irradiated ZnO is a manifestation of the radiation hardness of the material. With a fluence of  $\Phi = 6 \times 10^{17} \text{ cm}^{-2}$ , the introduction rate can be estimated as  $\Sigma_V = [V]/\Phi \approx 0.03 \text{ cm}^{-1}$ . This is a factor of 30 lower than determined for  $V_{\text{Ga}}$  in GaN [15]. As the introduction rates of primary defects are typically  $\approx 1 \text{ cm}^{-1}$ , only a very low fraction of Zn vacancies probably survive the recombination processes in the irradiation. Interestingly, no changes in the temperature dependent Hall or positron data were observed with a lower fluence than  $\Phi = 6 \times 10^{17} \text{ cm}^{-2}$ , also suggesting that secondary processes are present to induce nonlinear defect production.

In summary, we have combined temperature dependent Hall measurements and positron annihilation spectroscopy to study the acceptor defects in as-grown and electron irradiated ZnO. We showed that the zinc vacancy is the dominant acceptor defect in as-grown ZnO, which is  $n$ -type due to residual hydrogen impurities. In the electron irradiated material, Zn vacancies are also dominant but the negative ion-type defects introduced by irradiation also contribute significantly. Both of these defects have an introduction rate typical to secondary processes due to irradiation, manifesting the radiation hardness of ZnO.

We wish to thank T. A. Cooper for Hall-effect measurements and J. R. Sizelove for the Hall data fitting.

---

\*Electronic address: filip.tuomisto@hut.fi

- [1] D. C. Look *et al.*, Solid State Commun. **105**, 399 (1998).
- [2] D. C. Look *et al.*, Appl. Phys. Lett. **75**, 811 (1999).
- [3] S. F. J. Cox *et al.*, Phys. Rev. Lett. **86**, 2601 (2001).
- [4] D. M. Hofmann *et al.*, Phys. Rev. Lett. **88**, 045504 (2002).
- [5] C. G. Van de Walle, Phys. Rev. Lett. **85**, 1012 (2000).
- [6] F. A. Kröger, *The Chemistry of Imperfect Crystals* (North-Holland, Amsterdam, 1974).
- [7] A. F. Kohan *et al.*, Phys. Rev. B **61**, 15019 (2000).
- [8] R. M. de la Cruz *et al.*, Phys. Rev. B **45**, 6581 (1992).
- [9] A. Uedono *et al.*, J. Appl. Phys. **93**, 2481 (2003).
- [10] S. Brunner *et al.*, Mater. Sci. Forum **363**, 141 (2001).
- [11] D. C. Look, J. W. Hemsky, and J. R. Sizelove, Phys. Rev. Lett. **82**, 2552 (1999).
- [12] K. Saarinen, P. Hautojärvi, and C. Corbel, in *Identification of Defects in Semiconductors*, edited by M. Stavola (Academic Press, New York, 1998), p. 209.
- [13] K. Saarinen *et al.*, Phys. Rev. Lett. **79**, 3030 (1997).
- [14] S. Hautakangas *et al.*, Phys. Rev. Lett. **90**, 137402 (2003).
- [15] K. Saarinen *et al.*, Phys. Rev. B **64**, 233201 (2001).
- [16] M. Hakala, M. J. Puska, and R. M. Nieminen, Phys. Rev. B **57**, 7621 (1998).
- [17] K. Saarinen *et al.*, Appl. Phys. Lett. **75**, 2441 (1999).